Combining Analytical and Monte Carlo Modelling for Industrial Radiology

Carsten BELLON, Gerd-Rüdiger JAENISCH, Andreas DERESCH
BAM Bundesanstalt für Materialforschung und -prüfung, Berlin, Germany

Contact e-mail: Carsten.Bellon@bam.de

Abstract. Modelling becomes more and more important in modern NDE. It is increasingly used to optimize techniques for complex applications, to support the preparation of written procedures, and for education purposes. To describe the complete chain of RT, the model includes simulating all necessary properties of X- or Gamma-ray sources, the interaction of photons with material with special attention to scattered radiation, the detection process, and the complete geometrical RT setup handling arbitrary parts or constructions. Depending on the given inspection problem and the influencing factors that should be addressed by the simulation, an appropriate physical model has to be chosen to describe the underlying interaction mechanisms. The simulator aRTist combines analytical and Monte Carlo methods to efficiently model the radiation transport such that transmission as well as scatter techniques can be modelled. In this contribution we focus on Monte Carlo simulation of scatter contribution within aRTist. Examples for RT/tomographic applications and back-scatter techniques are presented to demonstrate the usability of the presented simulation tool for a broad range of radiological applications.

1 Introduction

Efficient and reliable non-destructive evaluation techniques are necessary to ensure the safe operation of complex parts and construction in an industrial environment. Radiation techniques are widely applied e.g. in industry. This includes projection techniques like classical radiography or tomography as well as scatter techniques. Over the years modelling has become more and more important in modern NDE. Computer simulation of radiation techniques can be used for different purposes in NDT, such as qualification of NDT systems, optimization of radiographic parameters, feasibility analysis, model-based data interpretation, and training of NDT/NDE personnel. Hence, computer modelling has to be able to handle all significant properties of an NDE system with sufficient accuracy. In the case of radiological applications, the model includes the radiation source, the interaction of radiation with material, the detection process, and the geometry of the part or the construction. As is known from practice, the latter can be very complex and requires a description allowing the handling of arbitrary geometries. The link between NDE models and CAD provides the ability to quantitatively evaluate complex inspections. Depending on the formulated inspection problem or the influencing factors that should be addressed by modelling, an appropriate physical model has to be chosen to describe the underlying interaction mechanisms.

Here the radiographic simulator *aRTist* [1,2] is presented which is an easy to use and practical simulation tool generating realistic radiographic images from virtual scenes. Test samples are geometrically represented by triangulated closed surfaces defining domains of homogeneous material. The used physical models from generation to detection of radiation allow for quantitative simulation results. An analytical calculation of the attenuation of radiation has been implemented by using an optimized ray tracer determining the lengths of the penetrated material segments. This yields close to real-time frame rates and allows for live preview.

The integrated Monte Carlo code *McRay* [3,4] completes the scattering model. As Monte Carlo calculations for complex geometries commonly demand extensive computational efforts, *McRay* has been specifically optimized for radiographic testing simulation and for linkage to *aRTist*. Thus it is usually a matter of seconds or minutes to simulate the scatter contribution in radiography using *McRay* on a personal desktop computer.

This paper presents two fundamental applications: (*i*) projection techniques like radiography and computed tomography, and (*ii*) back-scatter techniques when only one-sided access to the object is possible. First, *aRTist* and *McRay* are discussed in more detail. Then, the two examples are described and the results shown followed by concluding remarks.

2 Basics of *aRTist* and *McRay*

Modelling of radiation techniques basically considers four components: the radiation source, the interaction of radiation with matter, the detection of radiation, and the geometry of the object under investigation.

2.1 X-ray Source

X-rays are usually produced by the deceleration of high-energy electrons impinging on a metallic target. X-rays for most practical applications are generated in X-ray tubes, which consist of a cathode and an anode made from heavy metal with a high melting point. Electrons are emitted from the cathode and accelerated to the anode in a high-voltage electrical field. When the electrons hit the target of the X-ray tube the energy is transformed in several ways yielding the production of: (*i*) Bremsstrahlung with a continuous spectrum, (*ii*) characteristic radiation, and (*iii*) for most of the energy heat. The implemented model for X-ray sources [5-7] consists of a coupled semi-analytical description of Bremsstrahlung production and characteristic radiation emission based on fundamental interaction cross sections, describing electron and photon transport via numerical integration of discretized distributions. No free parameters are included in the model. It is capable of handling X-ray sources with thick targets including arbitrary beam geometry as well as transmission targets. Various target materials can be chosen.

2.2 Interaction Mechanisms

For the interaction of radiation with matter we restrict our model to photon interactions and do not account for electrons, which are also implemented in *McRay*. Accordingly the following interaction mechanisms are considered: the photoelectric effect, coherent and incoherent scattering, and for photon energies larger than 1 MeV pair production. To account for electron binding effects form factors and scattering functions are used for coherent and incoherent scattering. Additionally secondary effects such as X-ray fluorescence are considered.

The stationary Boltzmann equation (1) is used to model the photon transport

$$\boldsymbol{\Omega}\cdot\nabla I\left(\boldsymbol{r},E,\boldsymbol{\Omega}\right)+\mu\left(E\right)I\left(\boldsymbol{r},E,\boldsymbol{\Omega}\right)= \int_0^\infty \mathrm{d}E'\int_{4\pi}\mathrm{d}\Omega'\;\sigma\left(E'\rightarrow E,\boldsymbol{\Omega}'\rightarrow\boldsymbol{\Omega}\right)I\left(\boldsymbol{r},E',\boldsymbol{\Omega}'\right)+S\left(\boldsymbol{r},E,\boldsymbol{\Omega}\right) \tag{1}$$

It describes the variation of the photon flux $I(\boldsymbol{r},E,\boldsymbol{\Omega})$ at position $\boldsymbol{r}$ with direction $\boldsymbol{\Omega}$ and energy E. The left hand side of Eq. (1) accounts for the reduction of the flux by the interaction of photons with matter given by the linear attenuation coefficient $\mu(E)$

$$\mu\left(E\right)=\tau+\sigma_{\text{coherent}}+\sigma_{\text{incoherent}}+\pi \tag{2}$$

with the absorption coefficient τ, the scattering coefficients σ_{coherent} and $\sigma_{\text{incoherent}}$, and the pair production coefficient π. The right hand side describes the increase of the photon flux $I(\boldsymbol{r},E,\boldsymbol{\Omega})$ by scattering contributions from other energies E' and other directions $\boldsymbol{\Omega}'$ given by the scattering cross section $\sigma(E'\rightarrow E,\boldsymbol{\Omega}'\rightarrow\boldsymbol{\Omega})$ as well as by internal photon sources $S(\boldsymbol{r},E,\boldsymbol{\Omega})$ such as X-ray fluorescence or electron-positron annihilation.

If secondary and scatter contributions are neglected, i.e. the right hand side of eq. (1) vanishes, the remaining ordinary differential equation can be directly integrated leading to the attenuation law

$$I_p\left(\boldsymbol{r},\boldsymbol{\Omega},E\right)=I_0\left(\boldsymbol{r},\boldsymbol{\Omega},E\right)e^{-\int_0^{|\boldsymbol{r}-\boldsymbol{r}_0|}\mathrm{d}R\;\mu\left(\boldsymbol{r}-R\boldsymbol{\Omega},E\right)} \tag{3}$$

deriving the primary photon flux $I_p(\boldsymbol{r},E,\boldsymbol{\Omega})$ from the initial flux $I_0(\boldsymbol{r},E,\boldsymbol{\Omega})$, which carries the major information for radiographic techniques. Anyway, the contribution of scattered radiation has to be considered to compute the total intensity radiation I forming the projection image

$$I=I_p+I_s \tag{4}$$

with I_s being the scattered photon flux.

To simulate I_p an analytical calculation of the attenuated radiation has been implemented in *aRTist* by using an optimized ray tracer determining the lengths of the penetrated material segments. This yields close to real-time frame rates and allows for live preview.

For the scattered intensity, which also includes internal sources, two models are implemented in *aRTist*:

1. Build-up factor model assuming that the contribution of scattered radiation does not carry any information about the object under investigation, i.e. implemented as a constant offset depending on the average penetrated material thickness
2. Monte Carlo model *McRay* describing the interactions of photons with matter in detail and allowing the separation of the primary and scattered contribution to the total intensity

As Monte Carlo calculations for complex geometries commonly demand extensive computational efforts, *McRay* has been specifically developed for radiographic testing simulation and for linkage to *aRTist*. Thus it is usually a matter of seconds or minutes on a personal desktop computer to simulate the scatter contribution in radiography using *McRay*. For a more detailed description of the scatter contribution, e.g. for back-scatter techniques, the *McRay* calculation can be executed on a remote system (e.g. HPC cluster) if available.

2.3 Detector Response

Calculated or measured transmission functions are used in order to describe the conversion of photons registered by the detector and its response. The energy dependence of the response of a specific detector is thereby considered. *aRTist* provides a library for different detectors such as X-ray films, imaging plates, and digital detector arrays. Additionally, a module allowing the definition of detector characteristics is supplied with *aRTist*. The inner unsharpness is simulated by Gaussian filtering. Noise is added to the image pixel by pixel depending on its grey value.

2.4 Virtual Scene in aRTist

aRTist models a real inspection scenario by defining a virtual setup. Source and detector consist of raster points on a finite extended plane. Besides source and detector the geometrical computer model of the experimental setup has to support the representation of the test sample geometry. One or more geometrical part representations can be freely arranged in the virtual scene. Parts are described by a boundary representation of closed surfaces, which separate areas of homogeneous material. Facetted (triangulated) boundary descriptions are used in *aRTist*. Curved surfaces are approximated by an appropriate number of plane facets fitting to the accuracy requirements. For data exchange of this facetted part description the STL format can be used, which is a de-facto standard in the CAD domain. Several, interactively arrangeable part representations can easily be managed in the virtual 3D scene. Overlap of geometries in the scene and combination by Boolean operators leads to variable defect descriptions independent of the surrounding host material.

3 Examples

3.1 Radiography Simulation with aRTist and McRay

By selecting the scatter model *McRay* the scatter contribution is considered in radiographic simulation without the requirement to specify additional parameters. The steps of simulation including Monte Carlo scatter calculation are:

1. Source model
2. Analytical primary image
3. Separate primary and scatter images simulated with *McRay*
4. Adaptive anisotropic smoothing of scatter image
5. Scaling of scatter image based on correlation of both primary images
6. Summation of analytic primary and scaled *McRay* scatter image
7. Detector model

Optionally a scatter image can be calculated once and used for several simulations. This saves computation time in cases where the parameter changes barely affect the scatter contribution. If required a dedicated *aRTist* module gives extensive control over *McRay* calculations.

Fig. 1 shows a typical radiographic simulation result with *aRTist*. Left the virtual setup is given presenting the arrangement of the X-ray source (120 kV), the test object (aluminium casting, wall thickness range from 4 mm to 40 mm) and the detector (source-to-detector distance 220 mm). The center image gives the analytical primary image calculated with *aRTist* considering the attenuation of the radiation according to Eq. (3) only. On the right the scatter image is presented as calculated by the above presented algorithm (steps 1-5). By adding the primary and the scatter image the radiographic image is obtained which is not shown in the figure. For this example it is shown that the scatter from the part

contains geometrical information about the object that cannot be neglected. The geometrical structure of the object can be identified in the primary as well as in the scatter image. Therefore for objects with large wall thickness variations like for castings a detailed treatment of the scattered radiation is required.

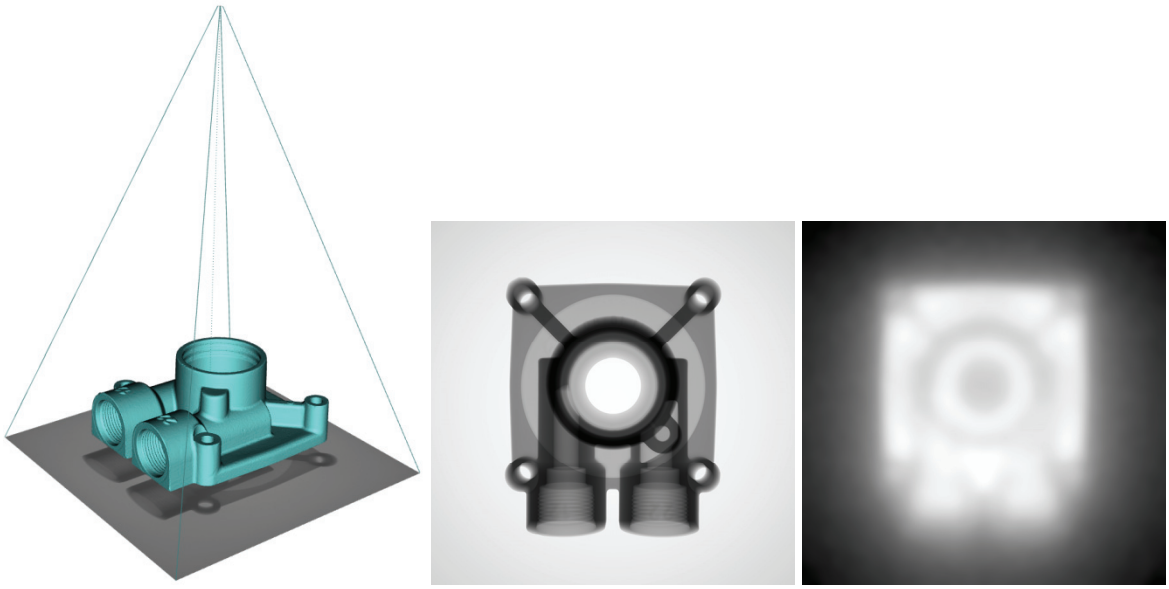

Fig. 1. Simulating radiography with *aRTist*: virtual setup (left); primary image (center); scatter image (right).

3.2 Simulation of Computerised Tomography with aRTist and McRay

aRTist also comes with a module for virtual computer tomography together with a standard back-projection algorithm for comparing the CT result with the original object and to investigate reasons for reconstruction artefacts. All tomography parameters can be freely chosen, such as the total rotation angle and the number of projections. This for example allows investigating limited angle and limited view applications. The module also allows grouping several objects for CT scan to separately handle the test object and possible flaws independently.

With *McRay* integrated, it is possible to account for scatter contributions from the test object, but also from non-rotating elements of the CT setup. To minimize the additional computational effort the *CTScan* module allows reusing one scatter image for a certain number of sequential projections.

Fig. 2 (top) shows the standard CT setup with the radiation source, the object under investigation, the rotation axis, and the detector. To demonstrate the capability of the *CTScan* module the same aluminium casting as in section 3.1 was used. Due to the different positioning of the object, the wall thickness ranges between 4 mm and 105 mm. Accordingly, the tube voltage was increased to 180 kV. The flat panel detector has 901×401 pixels. The source-to-detector distance was 370 mm. Fig. 2 (bottom) presents the primary image showing the internal structure of the object.

Fig. 3 (top) shows the scatter contribution to the projection data and Fig. 3 (bottom) a profile plot to compare the primary and scatter contribution. As it can be seen, the scatter intensity exceeds the primary one up to a factor of about 3. For the chosen setup the reconstruction results with (left) and without (right) scattered radiation are presented for one slice in Fig 4. Due to the large scatter contribution artifacts are found in the reconstruction considering the scatter contribution. The homogeneity of the object is not preserved.

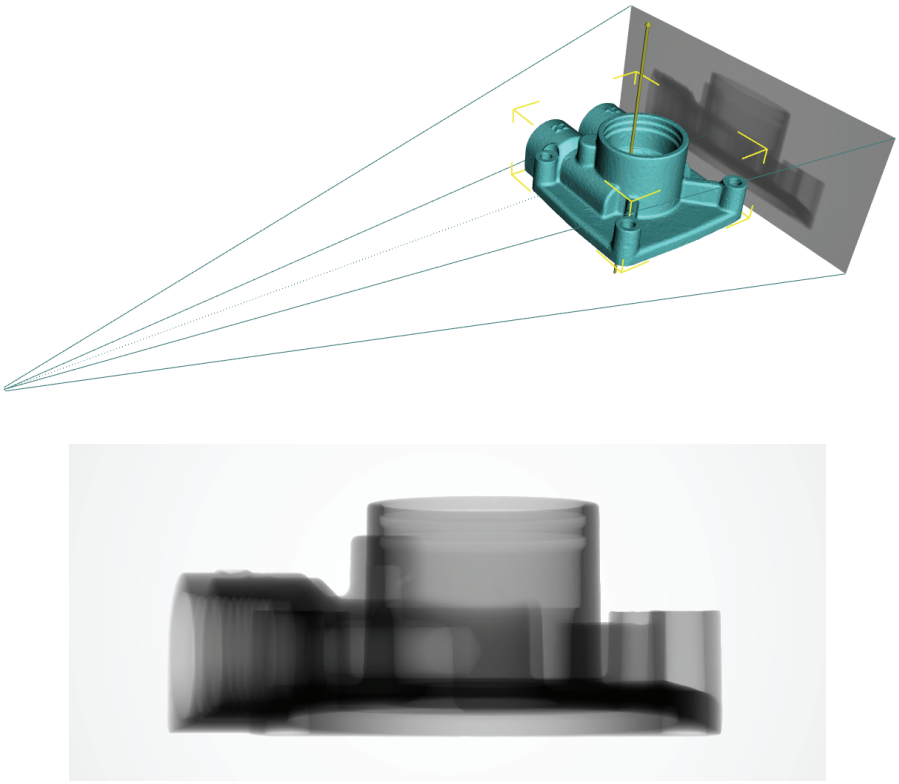

Fig 2. Simulating CT: virtual setup (top); primary image (bottom).

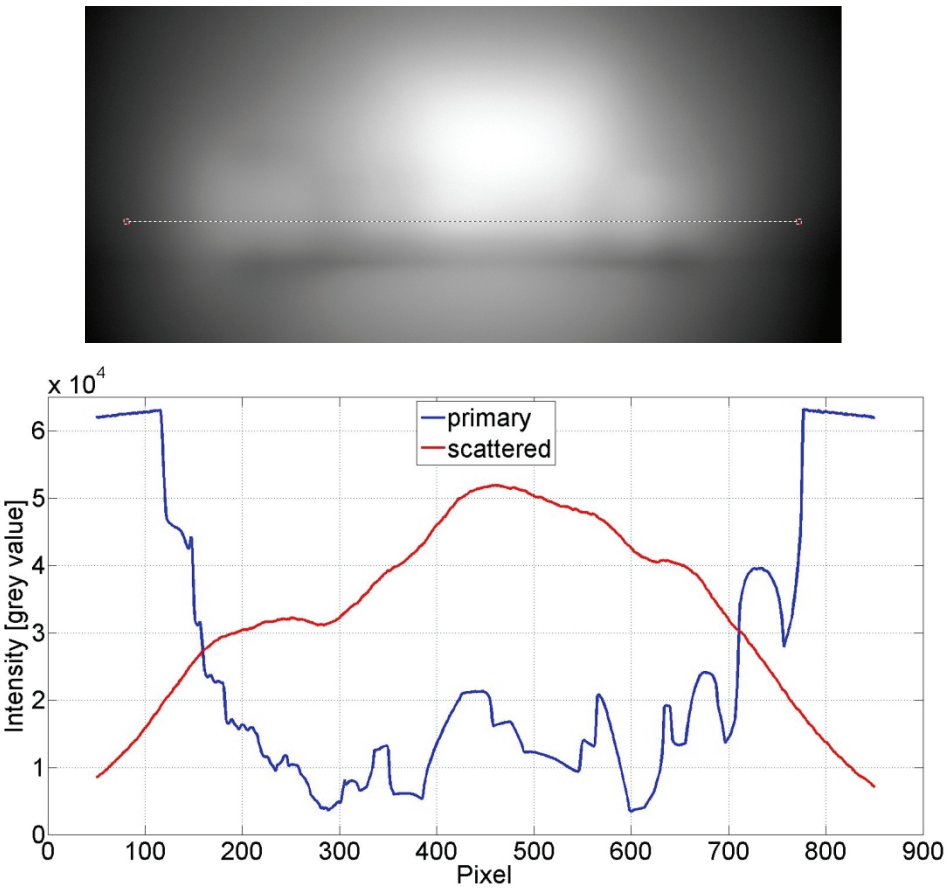

Fig. 3. Scatter image (top) and profile plot of primary and scattered contribution (bottom) at pixel line indicated in red (top).

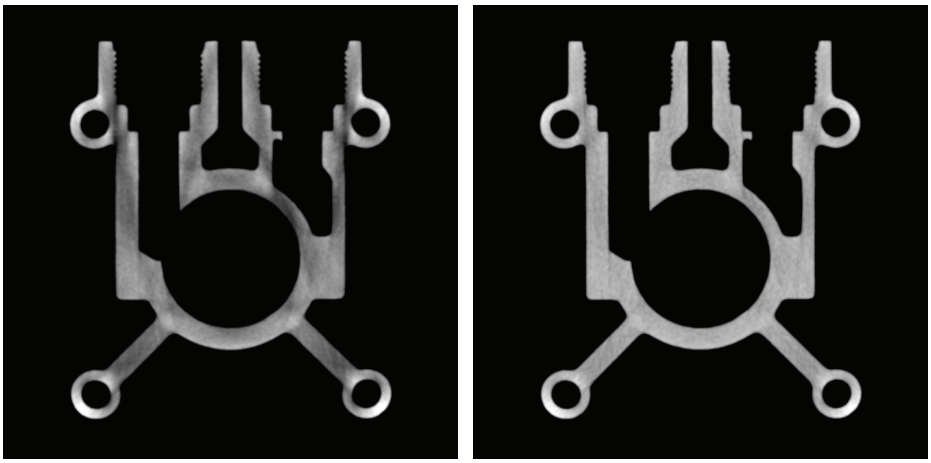

Fig. 4 Reconstruction with (left) and without (right) scattered radiation.

3.3 Back-Scatter Imaging with aRTist and McRay

The example presented here discusses the simulation of an imaging X-ray scatter technique using a back-scatter camera patented in [8]. Fig 5 shows the measurement setup for back scatter imaging with a bolt in front of a glass of water irradiated from the side (with image distortion caused by the camera design) arranged with *aRTist*. To illustrate the contribution to the back scatter image, Fig. 6 visualizes selected photon traces hitting the detector, calculated with *McRay*. Here the detector was shielded only from one side (Fig. 6 left) to demonstrate the contribution of scattering in air. Multiple scatter is clearly visible especially in the detailed view (Fig. 6 right). The final back scatter image is presented in Fig. 7.

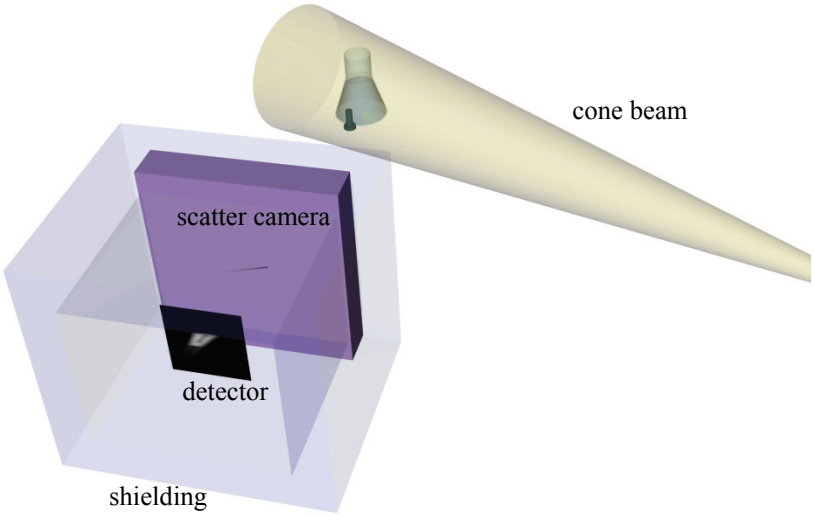

Fig. 5. *aRTist* virtual setup for back scatter imaging.

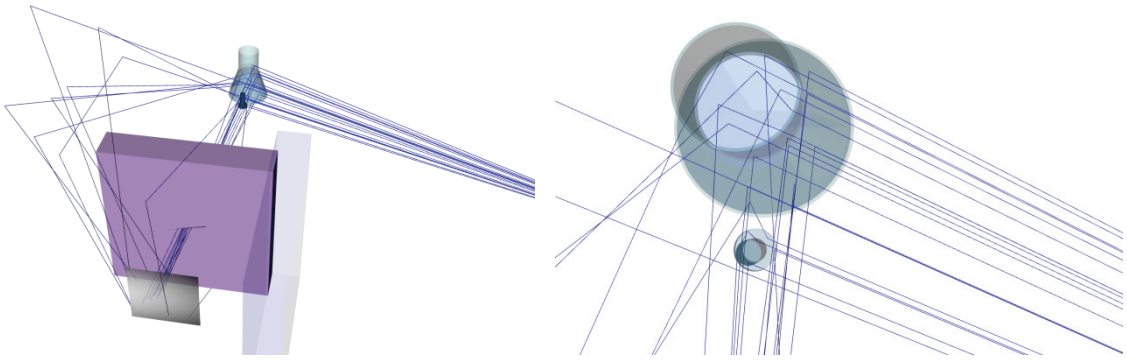

Fig. 6. Visualization of selected traces: overview image (left); detailed view (right).

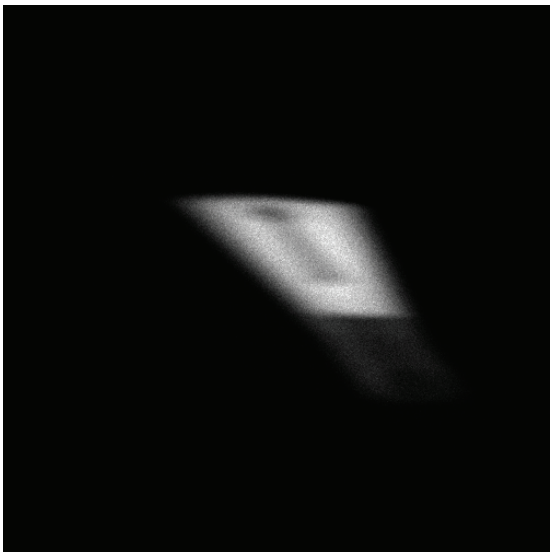

Figure 4: Back scatter image.

4 Conclusions

Radiography simulation with *aRTist* combining analytical and Monte Carlo methods has been presented. It was shown that the integrated Monte Carlo code *McRay* together with a specially developed smoothing procedure allows efficient calculation of the scatter contribution to radiographic images. Because of the implementation of *McRay*, optimized for projection techniques, this extension to simpler scatter models like built-up factor models is applicable on personal desktop computers.

The implemented *CTScan* module together with *McRay* allows accounting for scatter contributions not only from the test object, but also from non-rotating elements of the CT setup. One example has demonstrated the influence of scattered radiation on the final reconstruction result.

In addition the capability of *McRay* to simulate scatter imaging techniques has been shown. Here *aRTist* serves as graphical user interface for *McRay*. Because *McRay* is not optimized for back scatter applications, in this case it is recommended to run the simulations on a HPC cluster or other hardware allowing parallel computing.

References

[1] C. Bellon, A. Deresch, Ch. Gollwitzer, and G.-R. Jaenisch, 'Radiographic simulator aRTist: version 2', 18th WCNDT - World conference on nondestructive testing (Proceedings), pp 1-7 (Paper 333), 2012.

[2] C. Bellon and G.-R. Jaenisch, 'aRTist - Analytical RT Inspection Simulation Tool', DIR 2007 - International Symposium on Digital Industrial Radiology and Computed Tomography (Proceedings), pp 1-5, 2007.

[3] G.-R. Jaenisch, C. Bellon, U. Samadurau, M. Zhukovskiy, and S. Podoliako, 'McRay - A Monte Carlo Model Coupled to CAD for Radiation Techniques', 9th European Conference on NDT, 103-CD, pp 1-8, 2006.

[4] G.-R. Jaenisch, C. Bellon, U. Samadurau, M. Zhukovskiy, and S. Podoliako, 'Monte Carlo radiographic model with CAD-based geometry description', Insight Vol 48, No 10, pp 618-623, 2006.

[5] A. Deresch, G.-R. Jaenisch, C. Bellon, and A. Warrikhoff, 'Simulating X-ray spectra: from tube parameters to detector output', 18th WCNDT - World conference on nondestructive testing (Proceedings) pp 1-8 (Paper 336), 2012.

[6] A. Deresch, G.-R. Jaenisch, C. Bellon, and A. Warrikhoff, 'Simulation and experimental verification of X-ray spectra', Review of progress in quantitative nondestructive evaluation, American Institute of Physics, Vol 29 1211, pp 535-540, 2010.

[7] A. Deresch, C. Bellon, and G.-R. Jaenisch, 'A general spectrum model for X-ray generators', NDT & E International, Vol 79, pp 92-97, 2016.

[8] K. Osterloh et al., 'Schlitzkollimator für Röntgenrückstreu-Bildgebung', Patent, DE 10 2005 029 674, BAM